Interaction-Driven Giant Orbital Magnetic Moments in Carbon Nanotubes

Joshua O. Island,[1*] Marvin Ostermann,[1] Lee Aspitarte,[2] Ethan D. Minot,[2] Daniele Varsano,[3] Elisa Molinari,[3,4] Massimo Rontani,[3,†] and Gary A. Steele[1]

[1]*Kavli Institute of Nanoscience, Delft University of Technology, Lorentzweg 1, 2628 CJ Delft, Netherlands*
[2]*Department of Physics, Oregon State University, Corvallis, Oregon 97331, USA*
[3]*CNR-NANO, Via Campi 213a, 41125 Modena, Italy*
[4]*Dipartimento di Scienze Fisiche, Informatiche e Matematiche (FIM), Università degli Studi di Modena e Reggio Emilia, 41125 Modena, Italy*

(Received 12 January 2018; published 20 September 2018)

Carbon nanotubes continue to be model systems for studies of confinement and interactions. This is particularly true in the case of so-called "ultraclean" carbon nanotube devices offering the study of quantum dots with extremely low disorder. The quality of such systems, however, has increasingly revealed glaring discrepancies between experiment and theory. Here, we address the outstanding anomaly of exceptionally large orbital magnetic moments in carbon nanotube quantum dots. We perform low temperature magnetotransport measurements of the orbital magnetic moment and find it is up to 7 times larger than expected from the conventional semiclassical model. Moreover, the magnitude of the magnetic moment monotonically drops with the addition of each electron to the quantum dot directly contradicting the widely accepted shell filling picture of single-particle levels. We carry out quasiparticle calculations, both from first principles and within the effective-mass approximation, and find the giant magnetic moments can only be captured by considering a self-energy correction to the electronic band structure due to electron-electron interactions.

DOI: 10.1103/PhysRevLett.121.127704

A steady increase in the quality of carbon nanotube (CNT) devices has led to a deeper understanding of the physics that governs this material system that has captivated researchers for over two decades. This is particularly exemplified in the 2005 work by Cao *et al.* when they presented a method to fabricate ultraclean carbon nanotube transport devices whereby the nanotube was grown in the last step of fabrication [1]. This method greatly alleviated disorder brought on by defects, absorbed contaminants, and the underlying substrate [2,3]. The quality of similarly fabricated devices has lead to observations of elegant subtleties beyond early measurements of single electron tunneling such as an intimate coupling between spin and orbital motion [4], Wigner crystallization [5,6], and strong feedback between electron tunneling and mechanical motion [7]. While these experiments are a testament to the quality of ultraclean devices, they have increasingly offered glimpses of anomalous behavior which seem to persist without explanation [8].

In 2004, the orbital magnetic moment of electrons circling a carbon nanotube was shown to be a simple function of the nanotube diameter (D) and the electron's Fermi velocity (v_F), $\mu_{\mathrm{orb}} = De\nu_F/4$ (Ref. [9]). This relation has been supported by other works finding reasonable agreement between magnetotransport measurements of μ_{orb} and measurements of the average nanotube diameter for certain growth conditions [10,11]. Some works, however, find deviations from this relation where either measured μ_{orb}'s infer exceptionally large single wall nanotube diameters [4,12,13] (>3 nm) or the measurements of μ_{orb} and the nanotube diameter simply do not agree at all [14]. Deviations in the Fermi velocity, with reported experimental values of $(0.8\text{–}1.1) \times 10^6$ ms^{-1} (Refs. [15,16]), cannot account for the disagreement.

Reports of the magnitude of spin orbit coupling in carbon nanotube quantum dots have shown a similar trend. Spin orbit couplings as large as sixteen times greater than theoretical predictions have been measured [14,17]. A fraction of this discrepancy may lie in the use of the measured orbital magnetic moment to determine the nanotube diameter which, as we note above, can lead to discrepancies. Theory predicts Zeeman-like and orbital-like spin-orbit couplings of $\delta^0_{\mathrm{SO}} \approx -[0.3\ \mathrm{meV}/D\ (\mathrm{nm})] \cos 3\theta$ and $\delta^1_{\mathrm{SO}} \approx -[0.3\ \mathrm{meV}/D\ (\mathrm{nm})]$, respectively, θ being the chiral angle [8,18]. A larger inferred nanotube diameter would invariably lead to smaller theoretically predicted spin-orbit couplings.

Lastly, one of the long-standing mysteries in low temperature transport experiments on carbon nanotubes is a nonclosing or residual band gap at the Dirac field (closing field) for quasimetallic (small band gap) nanotubes. Theory says that metallic nanotubes can develop a band gap due to symmetry breaking of the underlying graphene lattice from strains, twists, and curvature. The magnitude of this gap is predicted to be around tens of millielectron volts but zero field gaps of an order of a magnitude larger have been reported [19–21]. Perhaps most intriguingly, though, in the

single-particle picture, these gaps should vanish at the Dirac field as the nanotube quantization line is pushed to the Dirac point of the underlying graphene band structure resulting in a truly metallic nanotube. In experiment this has not been observed and typically a residual gap exists of tens of millielectron volts. Deshpande *et al.* have interpreted this phenomenon in the context of a Mott insulating phase [22]. The extracted $1/R^{1.3}$ dependence, where R is the nanotube radius, however, relied on inferred nanotube diameters from the measured orbital magnetic moments.

Recent experiments from the present authors and others have shown that the nanotube band gap is extremely sensitive to the dielectric environment supporting indications of a strong role from interactions [20,23]. Emerging theory suggests the residual gap in narrow-gap nanotubes is the manifestation of an excitonic insulating phase, stabilized in the ground state by long-range Coulomb interaction, as electron-hole pairs spontaneously condense near the Dirac field where the transport gap should completely close [24,25]. The experimental signature of this exciting phase predicted over 50 years ago [26–30] is a slower decay of the residual gap as a function of the nanotube radius ($\Delta_{\mathrm{res}} \sim 1/R$) as compared with the predicted Mott gap decay ($\Delta_{\mathrm{res}} \sim 1/R^{1/(1-g)}$, with $g < 1$) (Ref. [25]). The true nanotube radius would be required to differentiate the two paradigms and elucidate the origin of the nonclosing gap.

Here, we report on orbital magnetic moments in ultraclean carbon nanotube quantum dots that deviate from existing theory both qualitatively and quantitatively. Instead of a magnetic moment which remains constant within a shell, we find that the orbital magnetic moment decreases monotonically with each added electron. Additionally, we analyze the magnitude of the moments and find that they are much larger than expected from semiclassical estimates based on a direct measurement of the nanotube diameter. We further compare our results with other models taking into account a change in the size of the quantum dot with filling, a change in charging energy with magnetic field, and the orbital magnetic moment of a Wigner molecule. None of these models suffice to explain the magnitude or trend of our observations. It is only by treating electrons added to the dot as quasiparticles dressed by the Coulomb interaction with other electrons already present in the nanotube, including those in the filled valence band, that we are able to account for the enhanced orbital magnetic moment. A self-energy correction to the gap computed within the effective-mass approximation results in good agreement between observations and theory and is further validated by a first-principles *GW* calculation for a small nanotube. Finally, in agreement with previous studies, we show that our small band gap tubes present a residual gap at the Dirac field and we discuss the implications of our results in the context of the Mott and excitonic insulating phases.

The fabrication of our ultraclean suspended devices follows from the process developed in Ref. [31] using a methane growth recipe detailed in Ref. [32]. Figure 1(b) shows a scanning electron microscopy image of a characteristic device (device *A*) after measurement. Note that this tube ruptured after measurement and before imaging. The nanotube can be seen at the location of the black arrows for the left trench. Low temperature measurements are performed in a dilution fridge at temperatures of 100 mK–4 K. We measure the current (I) as a function of two terminal voltage bias (V), back-gate voltage (V_g), and magnetic field (B). We measured four devices (labeled *A*–*D*) in detail having similar low temperature characteristics (see the Supplemental Material for additional devices [33]) and present one device (A) in the main text for consistency.

Results.—We now turn to the low temperature measurements of our carbon nanotube devices. Figure 1(a) shows a stability diagram of the calculated differential conductance (dI/dV) [from the measured current (I)] as a function of bias voltage V and back-gate voltage V_g for device *A*. The characteristic Coulomb blockade diamonds can be observed signaling the single electron transistor (SET) regime with a stable confinement of holes (on the left) and electrons (on the right) separated by a small energy band gap. The well-defined periodicity of the Coulomb diamonds and uniformity of the slopes indicate transport through a single defect-free carbon nanotube quantum dot. We observe orders of magnitude larger currents for holes than electrons [overlaid line profile in Fig. 1(a)] due to hole doping from the electrodes [31]. An estimate of the band gap can be made from subtracting the average addition energies (heights of diamonds on the left and right of the band gap, see Supplemental Material for a stability plot of low filling [33]) for the first hole and electron from the height of the central diamond [4]. For device *A* we estimate a zero field gap of ≈76 meV.

In the simplest picture, the electronic states in carbon nanotube quantum dots can be thought of as semiclassical orbits around the circumference of the tube giving circling electrons on the nanotube an orbital magnetic moment of $\mu_{\mathrm{orb}} = De\nu_F/4$ directed along the nanotube axis [9]. Upon application of a magnetic field along the tube axis, this orbital magnetic moment causes a shift in the energy of the electronic states of $\Delta E = -\boldsymbol{\mu}_{\mathrm{orb}} \cdot \mathbf{B} = \pm\mu_{\mathrm{orb}} B_{\parallel}$. The shift is either negative or positive depending on the orientation, clockwise or anticlockwise, of the circular orbits which correspond to electrons in the **K** or **K**' valley of the electronic band structure [9]. In the single-particle shell filling picture, two electrons (spin up and spin down) fill the lowest energy valley and the subsequent two electrons fill the next valley giving a total of four electrons per shell [46,47]. A straightforward estimate of the magnitude of the expected orbital magnetic moment for a carbon nanotube quantum dot can be made by measuring directly the nanotube diameter. For example, in Fig. 1(c) we show an

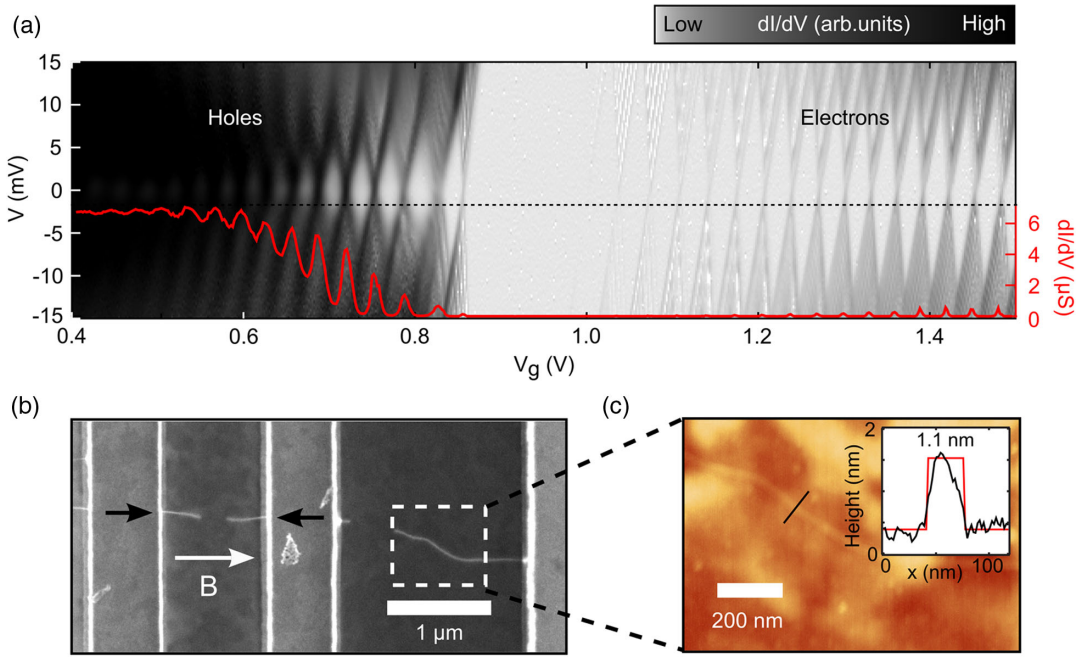

FIG. 1. (a) Gray-scale plot of (dI/dV) as a function of bias voltage (V) and gate voltage (V_g) at 3 K. The overlaid line cut shows (dI/dV) at a bias voltage of $V \approx -2$ mV. (b) Scanning electron microscopy (SEM) image of device A. Note that this tube ruptured after measurements and before imaging. Two trenches can be seen, one on the left where the nanotube is indicated with two black arrows and one on the right which was used for height analysis. (c) Atomic force microscopy (AFM) image of the same tube. The inset shows a line cut across the tube at the location of the black line in the AFM image.

atomic force microscopy (AFM) image of device A taken at the location indicated by the box in the scanning electron microscope (SEM) image in Fig. 1(b). For this tube having a relatively small diameter of 1.10 ± 0.03 nm (from five independent measurements of the tube), we expect an orbital magnetic moment of $\mu_{\rm orb} = 0.28 \pm 0.01$ meV/T for the first shell [see the Supplemental Material [33] for another device (B) having a larger diameter of 3.00 ± 0.04 nm and expected $\mu_{\rm orb}$ of 0.75 ± 0.01 meV/T].

In order to directly extract the experimental magnitude of the orbital magnetic moment, we apply a parallel component of the magnetic field along the nanotube axis [indicated in Fig. 1(b)] and measure the change in the energy of the ground state. The first four Coulomb peaks corresponding to the first shell of device A are shown in Fig. 2(a) and plotted as a function of magnetic field. The shift in energy of each level is related to the gate voltage through the factor $\alpha = |e|C_g/C_{\rm tot}$. Figure 2(b) shows the single electron tunneling (SET) regions for the first and second electronic ground states. The gate coupling is related to the positive (γ) and negative (β) slopes of the SET regions by $1/\alpha = 1/\beta + 1/\gamma$, with $\beta = |e|C_g/C_s$ and $\gamma = |e|C_g/(C_{\rm tot} - C_s)$, and where C_g, C_s, and $C_{\rm tot}$ are the gate, source, and total capacitances of the system. For the ground state charged with two electrons we calculate a gate coupling of $\alpha = 0.52$ eV/V. Using this coupling we plot the peak position, in energy, for the second electron from the data in Fig. 2(a) in Fig. 2(c). From a linear fit of this data from 0 to 3 T we estimate an orbital magnetic moment of $\mu_{\rm orb} \approx |dE/dB| = 1.42 \pm 0.03$ meV/T. The error here is to account for a possible deviation of $\pm 10°$ in the parallel component of the magnetic field.

In Fig. 2(d) we plot the measured $|dE/dB|$ (black filled circles) for the rest of the first shell of electrons. A maximum of 2.00 ± 0.04 meV/T is reached for the first electron and a monotonic decrease for subsequent filling of the first shell is observed. Not only is the absence of a switch to positive magnetic moment noted in Fig. 2(a) (i.e., the electrons seem to fall into one single valley), the magnitudes are much larger than expected. From the measured diameter, we estimated an orbital magnetic moment of $\mu_{\rm orb} = 0.28$ meV. This is 7 times smaller than the measured dE/dB for the first electron. We note that the expected Zeeman contribution of $\pm(1/2)g\mu_B B_{\|} = \pm 0.058 B_{\|}$ (meV) does not make up for the difference. In Fig. 2(d) (open squares) we plot the magnitude in energy for the next three electrons as well which are expected to stay constant within the shell. There is a clear disagreement between the single-particle model and the measured orbital magnetic moment. The measured moment for the first electron would correspond to a nanotube with a diameter of 8 nm in the semiclassical picture which exceeds the theoretical collapse threshold for single walled nanotubes of 5.1 nm [48]. In addition, chemical vapor deposition grown nanotubes rarely exceed 3 nm in diameter [49,50]. The disagreement between the data and semiclassical estimates from the measured

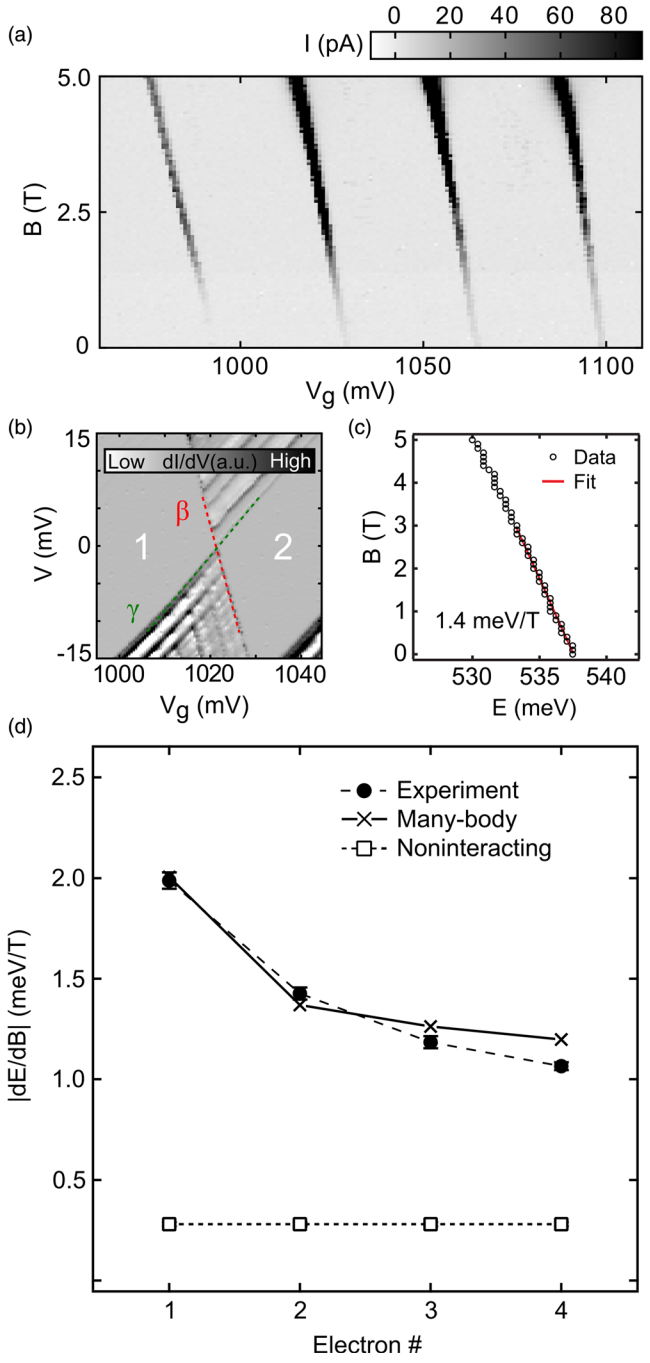

FIG. 2. (a) Measured current (I) at a bias voltage of 1 mV as a function of magnetic field. The first four Coulomb peaks are shown corresponding to the ground state for the first four electrons (the first shell) for device A ($T = 100$ mK). (b) Extraction of the voltage-to-energy conversion (α factor) from the Coulomb diamonds measured at 100 mK. (c) α-factor converted energy of the second electron as a function of field. The orbital magnetic moment is extracted by taking the slope of the change in the ground state energy with magnetic field. (d) Orbital magnetic moment for the first four electrons for device A. Black circles show the magnitude of the orbital magnetic moments extracted from the data in (a). Open squares show the semiclassical estimates from the measured diameter of the nanotube for device A [shown in Fig. 1(c)]. Crosses mark the results from our effective-mass GW calculations.

nanotube diameter is quite remarkable and encourages further investigation. In the Supplemental Material we first try to recover the enhancement through modifications of the semiclassical model given changes in the size of the quantum dot or the charging energies with magnetic field [33]. Neither effects account for our observed enhancement. The appearance of all four electrons filling a single valley is an indication of strong electron-electron interactions and the possible formation of a Wigner molecule [5,6,51]. We consider a simple model of electrons in the Wigner crystal regime in the Supplemental Material which again fails to reproduce our results [33]. We additionally note that three of the four devices show Wigner-like characteristics indicating strong interactions and one (device B) displays single-particle-like filling but still presents an enhanced orbital magnetic moment underlying the ubiquity of our results and failure of these simple models to reproduce them.

Instead, we adopt a different approach and consider the many-body correction to the noninteracting band gap induced by the quasiparticle self-energy that originates from electron-electron interactions [52,53]. We calculate the magnitude of the orbital magnetic moment within the GW scheme [52,53] and validate our predictions based on the effective mass approximation by investigating an additional case study from first principles [see Fig. 3(a) and Supplemental Material [33]]. We remark that our theory fully takes into account the gap-opening effect of tube curvature. The results of our effective mass calculations are shown in Fig. 2(d) along with the measured data for device A. Good agreement is found for both the magnitude and trend of the measured data. As electrons are added to the empty conduction band, the Coulomb interaction is effectively screened by the metal-like 1D Lindhard dielectric function leading to a monotonic decrease in the magnitude of the orbital magnetic moment (see Supplemental Material for details [33]). The qualitative phenomenon that we have observed, the dramatic change of the orbital moment upon adding a single electron to the shell, cannot be explained in a single-particle framework. This in itself is strong evidence for many-body effects in our device. The fact that we are able to reproduce this fundamentally non-single-particle phenomena using the presented first-principle GW calculations is an additional strong supporting piece of evidence that these orbital effects have their origin in many-body physics.

Finally, we note that, following similar studies [22], we observe the persistence of a nonclosing gap at the Dirac field which is not reproduced in our GW calculations. Figure 3(a) shows a representative first-principles calculation for the narrow-gap (9,0) zigzag tube as a function of the magnetic field. The latter is expressed in terms of the magnetic flux (ϕ) piercing the tube cross section to the flux quantum (ϕ_0), as we expect a qualitatively similar trend for all narrow-gap tubes, independent from their chirality. The black circles and red squares show, respectively, density functional theory (DFT, also labeled as

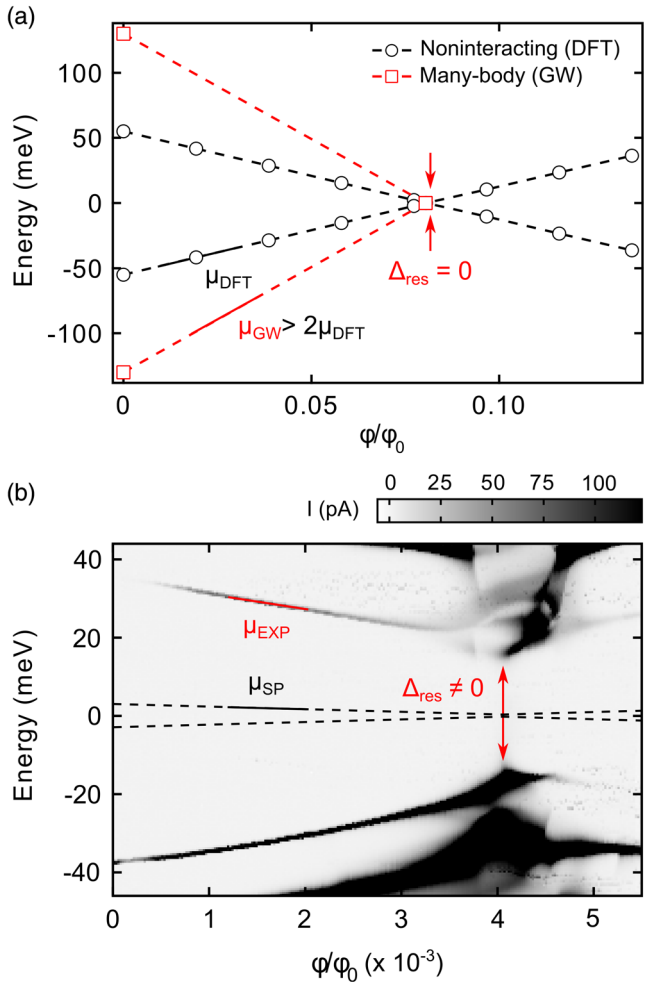

FIG. 3. (a) The ground state energy for the first electron (positive energy) and hole (negative energy) as a function of magnetic flux threading the nanotube to the flux quantum (ϕ_0) calculated from first principles for the narrow-gap (9,0) zigzag tube at the density functional theory (black open circles, "noninteracting") and *GW* (red open squares, "many-body") level. (b) Measured current for device *A* as a function of energy (converted from gate voltage using the α factor) and magnetic flux for the first electron (positive energy) and hole (negative energy).

noninteracting) and *GW* calculations (many-body) for the first electron and the first hole ground states. When accounting, from first principles, for the *GW* self-energy we find a considerable enhancement to the DFT band gap which leads to enhanced orbital magnetic moments and a steeper slope in the ground state energy as a function of magnetic field, essentially restating the effective-mass prediction of Fig. 2(d). Still, though, at high enough fields both first-principles and effective-mass *GW* calculations predict that the electron and hole ground states meet and the transport gap completely closes ($\Delta_{\mathrm{res}} = 0$). Figure 3(b) shows the ground state energy of the first electron and the first hole for device *A* to higher magnetic fields. It can be seen that at 9 T ($\approx 4 \times 10^{-3}\ \phi/\phi_0$) the two ground states reach the closest point before diverging at higher fields. Indeed, all four devices show the presence of a nonclosing gap at higher fields suggesting an additional contribution to the gap beyond the *GW* enhancement of the zero-field gap (see Supplemental Material [33]). We extract residual gaps (at the Dirac field) of $\Delta_{\mathrm{res}} = 34$, 38 meV and noninteracting gaps (change in gap energy from $B = 0$ T to $B = 9$ T) of $E = 42$, 17 meV for devices *A* and *B*, respectively, having diameters of 1.1 and 3 nm.

Two paradigms have been proposed to explain the presence of this residual gap at the Dirac field in ultraclean carbon nanotube devices, namely, the Mott insulator [22,54–59] and the excitonic insulator [24,25]. Our present study lacks the statistics required to differentiate the two paradigms which predict specific scalings with the nanotube diameter. However, we have shown here that direct measurements of the nanotube diameter are required as interactions in small band gap nanotubes result in enhanced orbital magnetic moments and discrepancies in inferred nanotube diameters.

Conclusion.—We have investigated observations of anomalous orbital magnetic moments in ultraclean carbon nanotube quantum dots. We find that the orbital magnetic moment is up to 7 times larger than expected from the semiclassical estimates. We analyze the possible influences on the orbital magnetic moment and find that the simplest corrections do not explain our results. We instead build a *GW* corrected effective mass model, supported by first-principle results, and find good agreement with our experimental orbital magnetic moment results. Our measurements suggest that the gapped electronic structure of nominally metallic CNTs is strongly modified by interaction-driven phenomena. These interactions are rapidly screened by adding a few electrons onto the CNT, which is reflected in the orbital magnetic moment. We note the presence of a nonclosing transport gap at higher magnetic fields which falls outside the scope of our developed model but highlights further interaction-driven phenomena. Our results emphasize the importance of interactions in ultraclean carbon nanotube quantum dots and provide the first steps toward closing similar long-standing open questions in low temperature transport studies.

The authors thank Herre van der Zant and Shahal Ilani for insightful discussions. We also acknowledge financial support by the Dutch Organization for Fundamental research (NWO/FOM). This work was supported in part by European Union H2020-EINFRA-2015-1 program under Grant No. 676598 project "MaX-Materials Design at the Exascale." E. D. M. and L. A. acknowledge support from the National Science Foundation under Grant No. 1151369. D. V., E. M., and M. R. acknowledge PRACE for awarding them access to the Marconi system based in Italy at CINECA (Grant No. Pre14_3622).

*jisland@physics.ucsb.edu
Present address: Department of Physics, University of California, Santa Barbara, California 93106, USA.
†massimo.rontani@nano.cnr.it

[1] J. Cao, Q. Wang, and H. Dai, Electron transport in very clean, as-grown suspended carbon nanotubes, Nat. Mater. **4**, 745 (2005).
[2] M. R. Amer, A. Bushmaker, and S. B. Cronin, The influence of substrate in determining the band gap of metallic carbon nanotubes, Nano Lett. **12**, 4843 (2012).
[3] J.-C. Charlier, Defects in carbon nanotubes, Acc. Chem. Res. **35**, 1063 (2002).
[4] F. Kuemmeth, S. Ilani, D. C. Ralph, and P. L. McEuen, Coupling of spin and orbital motion of electrons in carbon nanotubes, Nature (London) **452**, 448 (2008).
[5] V. V. Deshpande and M. Bockrath, The one-dimensional Wigner crystal in carbon nanotubes, Nat. Phys. **4**, 314 (2008).
[6] S. Pecker, F. Kuemmeth, A. Secchi, M. Rontani, D. C. Ralph, P. L. McEuen, and S. Ilani, Observation and spectroscopy of a two-electron Wigner molecule in an ultraclean carbon nanotube, Nat. Phys. **9**, 576 (2013).
[7] G. A. Steele, A. K. Hüttel, B. Witkamp, M. Poot, H. B. Meerwaldt, L. P. Kouwenhoven, and H. S. J. van der Zant, Strong coupling between single-electron tunneling and nanomechanical motion, Science **325**, 1103 (2009).
[8] E. A. Laird, F. Kuemmeth, G. A. Steele, K. Grove-Rasmussen, J. Nygård, K. Flensberg, and L. P. Kouwenhoven, Quantum transport in carbon nanotubes, Rev. Mod. Phys. **87**, 703 (2015).
[9] E. D. Minot, Y. Yaish, V. Sazonova, and P. L. McEuen, Determination of electron orbital magnetic moments in carbon nanotubes, Nature (London) **428**, 536 (2004).
[10] A. Makarovski, A. Zhukov, J. Liu, and G. Finkelstein, SU(2) and SU(4) Kondo effects in carbon nanotube quantum dots, Phys. Rev. B **75**, 241407 (2007).
[11] H. O. H. Churchill, A. J. Bestwick, J. W. Harlow, F. Kuemmeth, D. Marcos, C. H. Stwertka, S. K. Watson, and C. M. Marcus, Electron-nuclear interaction in 13C nanotube double quantum dots, Nat. Phys. **5**, 321 (2009).
[12] P. Jarillo-Herrero, J. Kong, H. S. J. Van der Zant, C. Dekker, L. P. Kouwenhoven, and S. De Franceschi, Electronic Transport Spectroscopy of Carbon Nanotubes in a Magnetic Field, Phys. Rev. Lett. **94**, 156802 (2005).
[13] T. S. Jespersen, K. Grove-Rasmussen, K. Flensberg, J. Paaske, K. Muraki, T. Fujisawa, and J. Nygård, Gate-Dependent Orbital Magnetic Moments in Carbon Nanotubes, Phys. Rev. Lett. **107**, 186802 (2011).
[14] G. A. Steele, F. Pei, E. A. Laird, J. M. Jol, H. B. Meerwaldt, and L. P. Kouwenhoven, Large spin-orbit coupling in carbon nanotubes, Nat. Commun. **4**, 1573 (2013).
[15] S. G. Lemay, J. W. Janssen, M. van den Hout, M. Mooij, M. J. Bronikowski, P. A. Willis, R. E. Smalley, L. P. Kouwenhoven, and C. Dekker, Two-dimensional imaging of electronic wavefunctions in carbon nanotubes, Nature (London) **412**, 617 (2001).
[16] K.-C. Chuang, R. S. Deacon, R. J. Nicholas, K. S. Novoselov, and A. K. Geim, Cyclotron resonance of electrons and holes in graphene monolayers, Phil. Trans. R. Soc. A **366**, 237 (2008).
[17] S. H. Jhang, M. Marganska, Y. Skourski, D. Preusche, B. Witkamp, M. Grifoni, H. van der Zant, J. Wosnitza, and C. Strunk, Spin-orbit interaction in chiral carbon nanotubes probed in pulsed magnetic fields, Phys. Rev. B **82**, 041404 (2010).
[18] V. V. Maslyuk, R. Gutierrez, and G. Cuniberti, Spin-orbit coupling in nearly metallic chiral carbon nanotubes: A density-functional based study, Phys. Chem. Chem. Phys. **19**, 8848 (2017).
[19] J. O. Island, V. Tayari, S. Yiğen, A. C. McRae, and A. R. Champagne, Ultra-short suspended single-wall carbon nanotube transistors, Appl. Phys. Lett. **99**, 243106 (2011).
[20] L. Aspitarte, D. R. McCulley, A. Bertoni, J. O. Island, M. Ostermann, M. Rontani, G. A. Steele, and E. D. Minot, Giant modulation of the electronic band gap of carbon nanotubes by dielectric screening, Sci. Rep. **7**, 8828 (2017).
[21] A. C. McRae, V. Tayari, J. M. Porter, and A. R. Champagne, Giant electron-hole transport asymmetry in ultra-short quantum transistors, Nat. Commun. **8**, 15491 (2017).
[22] V. V. Deshpande, B. Chandra, R. Caldwell, D. S. Novikov, J. Hone, and M. Bockrath, Mott insulating state in ultraclean carbon nanotubes, Science **323**, 106 (2009).
[23] H. Lin, J. Lagoute, V. Repain, C. Chacon, Y. Girard, J.-S. Lauret, F. Ducastelle, A. Loiseau, and S. Rousset, Many-body effects in electronic bandgaps of carbon nanotubes measured by scanning tunnelling spectroscopy, Nat. Mater. **9**, 235 (2010).
[24] M. Rontani, Anomalous magnetization of a carbon nanotube as an excitonic insulator, Phys. Rev. B **90**, 195415 (2014).
[25] D. Varsano, S. Sorella, D. Sangalli, M. Barborini, S. Corni, E. Molinari, and M. Rontani, Carbon nanotubes as excitonic insulators, Nat. Commun. **8**, 1461 (2017).
[26] N. F. Mott, The transition to the metallic state, Philos. Mag. **6**, 287 (1961).
[27] R. S. Knox, *Solid State Physics, Suppl. 5: Theory of Excitons* (Academic Press, New York, 1963).
[28] L. V. Keldysh and Y. V. Kopaev, Possible instability of semimetallic state toward Coulomb interaction, Sov. Phys. Solid State **6**, 2219 (1965).
[29] D. Jérome, T. M. Rice, and W. Kohn, Excitonic insulator, Phys. Rev. **158**, 462 (1967).
[30] D. Sherrington and W. Kohn, Speculations about grey tin, Rev. Mod. Phys. **40**, 767 (1968).
[31] B. H. Schneider, S. Etaki, H. S. J. van der Zant, and G. A. Steele, Coupling carbon nanotube mechanics to a superconducting circuit, Sci. Rep. **2**, 599 (2012).
[32] G. A. Steele, G. Gotz, and L. P. Kouwenhoven, Tunable few-electron double quantum dots and Klein tunnelling in ultraclean carbon nanotubes, Nat. Nanotechnol. **4**, 363 (2009).
[33] See Supplemental Material at http://link.aps.org/supplemental/10.1103/PhysRevLett.121.127704 for additional devices (*B*, *C*, and *D*) which display similar characteristics as device *A* in the main text, a stability plot for device *A* at low filling (first four electrons and holes), a discussion and results on modifications to the semiclassical estimate of the orbital magnetic moment, a discussion and results on the orbital magnetic moment of a carbon nanotube Wigner crystal, and complete details on calculations of the orbital

magnetic moment within the *GW* scheme, which includes Refs. [34–45].

[34] T. Ando, Excitons in carbon nanotubes, J. Phys. Soc. Jpn. **66**, 1066 (1997).

[35] P. Giannozzi, S. Baroni, N. Bonini, M. Calandra, R. Car, C. Cavazzoni, D. Ceresoli, G. L. Chiarotti, M. Cococcioni, I. Dabo, A. Dal Corso, S. de Gironcoli, S. Fabris, G. Fratesi, R. Gebauer, U. Gerstmann, C. Gougoussis, A. Kokalj, M. Lazzeri, L. Martin-Samos *et al.*, Quantum ESPRESSO: A modular and open-source software project for quantum simulations of materials, J. Phys. Condens. Matter **21**, 395502 (2009).

[36] J. P. Perdew and A. Zunger, Self-interaction correction to density-functional approximations for many-electron systems, Phys. Rev. B **23**, 5048 (1981).

[37] T. Miyake and S. Saito, Band-gap formation in $(n, 0)$ single-walled carbon nanotubes ($n = 9$, 12, 15, 18): A first-principles study, Phys. Rev. B **72**, 073404 (2005).

[38] A. Marini, C. Hogan, M. Grüning, and D. Varsano, YAMBO: An *ab initio* tool for excited state calculations, Comput. Phys. Commun. **180**, 1392 (2009).

[39] R. W. Godby and R. J. Needs, Metal-Insulator Transition in Kohn-Sham Theory and Quasiparticle Theory, Phys. Rev. Lett. **62**, 1169 (1989).

[40] F. Bruneval and X. Gonze, Accurate *GW* self-energies in a plane-wave basis using only a few empty states: Towards large systems, Phys. Rev. B **78**, 085125 (2008).

[41] C. A. Rozzi, D. Varsano, A. Marini, E. K. U. Gross, and A. Rubio, Exact Coulomb cutoff technique for supercell calculations, Phys. Rev. B **73**, 205119 (2006).

[42] D. Sangalli and A. Marini, Anomalous Aharonov-Bohm gap oscillations in carbon nanotubes, Nano Lett. **11**, 4052 (2011).

[43] M. Abramowitz and I. A. Stegun, *Handbook of Mathematical Functions* (Dover, New York, 1972).

[44] G. F. Giuliani and G. Vignale, *Quantum Theory of the Electron Liquid* (Cambridge University Press, Cambridge, U.K., 2005).

[45] C. D. Spataru, Electronic and optical gap renormalization in carbon nanotubes near a metallic surface, Phys. Rev. B **88**, 125412 (2013).

[46] W. Liang, M. Bockrath, and H. Park, Shell Filling and Exchange Coupling in Metallic Single-Walled Carbon Nanotubes, Phys. Rev. Lett. **88**, 126801 (2002).

[47] S. Sapmaz, P. Jarillo-Herrero, L. P. Kouwenhoven, and H. S. J. van der Zant, Quantum dots in carbon nanotubes, Semicond. Sci. Technol. **21**, S52 (2006).

[48] M. He, J. Dong, K. Zhang, F. Ding, H. Jiang, A. Loiseau, J. Lehtonen, and E. I. Kauppinen, Precise determination of the threshold diameter for a single-walled carbon nanotube to collapse, ACS Nano **8**, 9657 (2014).

[49] J. Kong, A. M. Cassell, and H. Dai, Chemical vapor deposition of methane for single-walled carbon nanotubes, Chem. Phys. Lett. **292**, 567 (1998).

[50] G. Chen, Y. Seki, H. Kimura, S. Sakurai, M. Yumura, K. Hata, and D. N. Futaba, Diameter control of single-walled carbon nanotube forests from 1.3–3.0 nm by arc plasma deposition, Sci. Rep. **4**, 3804 (2014).

[51] A. Secchi and M. Rontani, Wigner molecules in carbon-nanotube quantum dots, Phys. Rev. B **82**, 035417 (2010).

[52] L. Hedin and S. O. Lundqvist, Effects of electron-electron and electron-phonon interactions on the one-electron states of solids, Solid State Phys. **23**, 1 (1969).

[53] G. Onida, L. Reining, and A. Rubio, Electronic excitations: Density-functional versus many-body Green's function approaches, Rev. Mod. Phys. **74**, 601 (2002).

[54] C. Kane, L. Balents, and M. P. A. Fisher, Coulomb Interactions and Mesoscopic Effects in Carbon Nanotubes, Phys. Rev. Lett. **79**, 5086 (1997).

[55] A. A. Nersesyan and A. M. Tsvelik, Coulomb blockade regime of a single-wall carbon nanotube, Phys. Rev. B **68**, 235419 (2003).

[56] A. A. Odintsov and H. Yoshioka, Universality of electron correlations in conducting carbon nanotubes, Phys. Rev. B **59**, R10457 (1999).

[57] H.-H. Lin, Correlation effects of single-wall carbon nanotubes in weak coupling, Phys. Rev. B **58**, 4963 (1998).

[58] Yu A. Krotov, D.-H. Lee, and S. G. Louie, Low Energy Properties of (n, n) Carbon Nanotubes, Phys. Rev. Lett. **78**, 4245 (1997).

[59] L. Balents and M. P. A. Fisher, Correlation effects in carbon nanotubes, Phys. Rev. B **55**, R11973 (1997).